Filler effects on the thermomechanical response of stretched rubbers

Jose Ricardo Samaca Martinez, Jean-Benoit Le Cam, Xavier Balandraud, Evelyne Toussaint, Julien Caillard

Filler effects on the thermomechanical response of stretched rubbers

J.R. Samaca Martinez
Clermont Université, Université Blaise Pascal, Institut Pascal, Clermont-Ferrand, France
CNRS, UMR 6602, Institut Pascal, Aubière, France
Michelin, CERL Ladoux, Clermont-Ferrand, France

J.-B. Le Cam
Université de rennes 1, LARMAUR ERL CNRS 6274, Campus de Beaulieu, Rennes, France

X. Balandraud
CNRS, UMR 6602, Institut Pascal, Aubière, France
Clermont Université, Institut Français de Mécanique Avancée, Institut Pascal, Clermont-Ferrand, France

E. Toussaint
Clermont Université, Université Blaise Pascal, Institut Pascal, Clermont-Ferrand, France
CNRS, UMR 6602, Institut Pascal, Aubière, France

J. Caillard
Michelin, CERL Ladoux, Clermont-Ferrand, France

ABSTRACT: This paper deals with the calorimetric analysis of deformation processes in filled styrene-butadiene rubbers. Heat sources produced or absorbed by the material due to deformation processes are deduced from temperature fields by using the heat diffusion equation. First, the results show that no mechanical (intrinsic) dissipation is detected for weakly filled SBR, meaning that the heat produced and absorbed over one mechanical cycle is the same whatever the stretch ratio reached. Second, the mechanical dissipation in highly filled and "demullinized" SBR is significant. The quantitative analysis carried out highlights the fact that it increases quasi-linearly with the stretch ratio. Finally, a simplified framework is proposed to discuss the identification of the heat sources, in particular the mechanical dissipation.

1 INTRODUCTION

Elastomers are widely used in industrial and research applications, mainly due to their ability to undergo large deformations without any damage, and to their damping properties. Nevertheless, due to their poor thermal conductivity, such materials are subjected to significant self-heating during stretching, all the more so if they are reinforced by fillers.

In this study, Infrared Thermography (IRT) is used to investigate the effects of fillers on the thermomechanical response of Styrene-Butadiene Rubber (SBR). IRT is a full thermal field measurement technique that provides accurate information about temperature variations at the surface of a specimen subjected to solicitations that can differ in nature (mechanical, thermal, chemical…). The temperature changes are due to the material response (heat source due to thermoelasticity, viscosity, phase changes, strain-induced crystallization, damage…) as well as structure effects (heat conduction and heat exchanges with the environment outside the specimen under study). Thus, due to heat conduction and heat exchanges, temperature is not a relevant quantity (see for example Chrysochoos & Louche (2000) and Chrysochoos et al. (2010)). For instance, temperature variation does not enable us to determine the characteristic strains at which strong exo- or endothermal phenomena occur, typically chain crystallization and crystallite melting (see for example Samaca Martinez et al. (2013a)).

This is the reason why thermal analysis has widely been extended to quantitative calorimetry (see for instance Samaca Martinez et al. (2013b)). For this purpose, the framework of the Thermodynamics of Irreversible Processes (TIP) and the heat diffusion equation are used. This approach enables us to measure the total heat source produced or

absorbed by the material. Under certain hypotheses, it is also possible to distinguish the part due to the thermomechanical couplings, which includes in particular thermoelastic couplings, from the part due to mechanical dissipation. This approach is used in the present study in order to determine the variation in mechanical dissipation due to filler effects in a SBR whose mechanical behaviour is stabilized, i.e. "demullinized". The mechanical dissipation is here expected to be only due to viscosity, not to the Mullins effect.

The paper is composed of two parts. The first part presents the experimental set-up. The second part presents the results, analysis and discussion. Concluding remarks close the paper.

2 EXPERIMENTAL SETUP

2.1 *Material and specimen geometry*

The materials considered here were SBR filled with two different amounts of carbon black, 5 and 50 phr (part per hundred of rubber in weight), they are denoted SBR5 and SBR50 respectively in the following. As shown in Table 1, apart from the filler quantity, their formulations were the same. It should be noted that these material formulations do not lead to stress-induced crystallization, unlike natural rubber, for instance.

Table 1. Chemical composition in parts per hundred rubber (phr).

Ingredient	SBR5	SBR50
Styrene-Butadiene Rubber (SBR)	100	100
Carbon black	5	50
Antioxidant 6PPD	1.9	1.9
Stearic acid	2	2
Zinc oxide ZnO	2.5	2.5
Accelerator CBS	1.6	1.6
Sulfur solution 2H	1.6	1.6

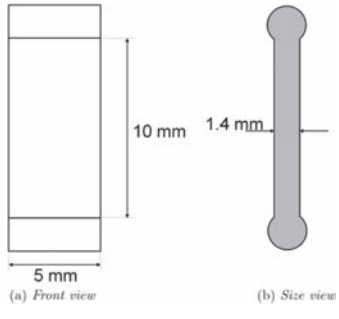

Figure 1. Specimen geometry.

The specimen geometry is presented in Figure 1. It was a thin dumbbell-shaped specimen, whose width, height and thickness were equal to 5 mm, 10 mm and 1.4 mm respectively. It can be noted that the width was chosen to ensure the homogeneity of the mechanical fields during uniaxial tensile tests, i.e. a uniaxial tension state.

2.2 *Loading conditions*

The mechanical loading corresponded to uniaxial cyclic loading. It was applied under prescribed displacement using an INSTRON 5543 testing machine. The signal shape was triangular in order to ensure a constant strain rate during loading and unloading. The loading and nominal strain rates were equal to ±300 mm/min and ±0.5 s^{-1}, respectively. The test corresponded to series of three cycles at four increasing maximum stretch ratios, defined as the ratios between the current and the initial length of the specimen. The maximum stretch ratio levels were chosen as follows:

- For the SBR5, the four maximum stretch ratios were $\lambda_1 = 2$, $\lambda_2 = 3$, $\lambda_3 = 3.5$ and $\lambda_4 = 4$, as shown in Figure 2(a).
- For the SBR50, the four maximum stretch ratios were $\lambda_1 = 2$, $\lambda_2 = 3$, $\lambda_3 = 4$ and $\lambda_4 = 4.5$, as shown in Figure 2(b).

λ_3 and λ_4 slightly differed from one formulation to the other, due to the fact that the stretches at failure were different (4.2 for SBR5 and 4.8 for SBR50).

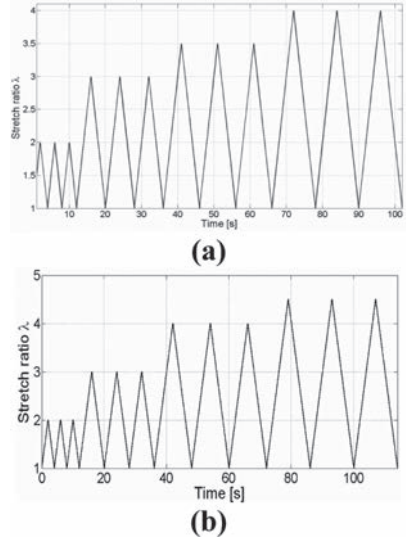

Figure 2. Mechanical loading conditions: (a) SBR5; (b) SBR50.

2.3 *Temperature field measurement*

Temperature field measurements were performed using a Cedip Jade III-MWIR infrared camera, which features a local plane array of 320 × 240 pixels and detectors with a wavelength range of 3.5–5 µm. Integration time was equal to 1500 µs. The acquisition frequency f_a was 147 Hz. The thermal resolution, namely the noise-equivalent temperature difference, was equal to 20 mK for a temperature range of 5–40 °C. The calibration of the camera detectors was performed with a black body using a Non-Uniformity Correction (NUC) procedure. During the measurement, the external heat sources were reduced by using a black box surrounding the specimen, featuring a small window for the IR camera to be able to observe the gauge zone of the specimen. The thermal quantity considered in the present study was the mean temperature variation of a small zone at the centre of the specimen. This quantity was obtained by subtracting the initial temperature from the current one, after applying a suitable movement compensation technique (Samaca Martinez et al., 2013a) to track this small zone during the test.

2.4 *Heat source calculation*

The heat sources produced or absorbed by the material itself were studied within the framework of the thermodynamics of irreversible processes. Considering the first and second principles of thermodynamics and assuming Fourier's law to model heat conduction (Germain et al., 1983; Boccara, 1968), the heat diffusion equation is written:

$$\rho C_{E,Vk}\,\dot{T} - \operatorname{div}\left(K \operatorname{grad} T\right) - r = s_h \tag{1}$$

$$\text{with } s_h = d_1 + S_{TMC} \tag{2}$$

where:

- s_h and r are the heat source produced or absorbed by the material due to stretch and the external heat source (e.g. by radiation), respectively;
- d_1 and S_{TMC} are the mechanical dissipation (always positive) and the heat source due to the thermomechanical couplings, respectively. In particular, the latter contains the thermoelastic coupling term mainly composed of so-called entropic coupling. The former is related to any irreversible mechanical phenomenon;
- ρ, K and $C_{E,Vk}$ are the density, the thermal conductivity tensor and the specific heat at constant strain E and internal state variables V_k, respectively.

This equation applies both in the reference configuration as well as in the current configuration, provided that we give a suitable definition of symbols r, div, K, grad, r and s_h. However, it is only in Lagrangian variables that the total derivative $\dot{T}$ can be calculated as a partial derivative. The temperature fields were measured at the surface of a flat specimen by an IR camera. As the tests performed were assumed to be homogeneous in terms of strain and stress, and as rubbers have a very low thermal diffusivity, the temperature fields were nearly homogeneous. Therefore the 3D heat diffusion equation (1) can be reduced to a "0D" formulation as shown in Chrysochoos & Louche (2000), Samaca Martinez et al. (2013b) and Chrysochoos (1995). In this case, the heat diffusion equation can be rewritten:

$$\rho C_{E,Vk}\left(\dot{\theta} + \frac{\theta}{\tau}\right) = s_h \tag{3}$$

where θ is the temperature variation from the initial temperature (here considered in the unstretched state at the beginning of the test). In this equation, τ is a characteristic time that accounts for the heat exchange with the outside environment. In practice, it can be experimentally determined by identification from a natural return to ambient temperature. For the present experiments, the characteristic time τ was defined as (40.50–3.25 λ) seconds, a formula obtained from experiments with λ varying between 1 and 6.

Lastly, the heat source s_h is divided by the product $\rho C_{E,Vk}$, leading to a quantity s in °C/s:

$$s = \frac{s_h}{\rho C_{E,Vk}} = \dot{\theta} + \frac{\theta}{\tau} \tag{4}$$

In the following, the ratio $s_h / \rho C_{E,Vk}$ will be named "heat source s" for the sake of simplicity. This equation will be used to calculate the heat source s from the temperature variation θ.

3 RESULTS

Figure 3 presents the nominal stress, defined as the force per unit initial surface, *versus* the stretch ratio,

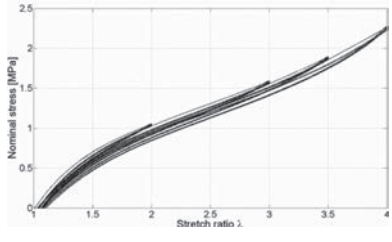

Figure 3. Mechanical response of SBR5.

for the SBR5. This figure shows that mechanical cycles have little effect on the mechanical response, in the sense that neither significant stress softening nor a hysteresis loop are observed. Finally, it should be noted that a residual strain is observed. It can reach 10% for the maximum stretch ratio applied.

Figure 4 presents the results obtained in terms of the heat source *versus* the applied stretch ratio, for SBR5. Figures. 4(a), (b), (c) and (d) present the results for $\lambda_1 = 2$, $\lambda_2 = 3$, $\lambda_3 = 3.5$ and $\lambda_4 = 4$, respectively. The unbroken lines correspond to the heat sources calculated on loading and unloading. The dotted line corresponds to the absolute value of the heat sources on unloading. This curve is plotted in order to compare the heat sources produced and absorbed during loading and unloading. These figures show that the absolute value of the heat sources has the same evolution during loading and unloading, highlighting the fact that no mechanical dissipation is detected. Indeed, mechanical dissipation d_1 is always a positive quantity, for loading as well as for unloading. If d_1 had been different from zero during a load-unload cycle, the curves would be asymmetrical. Consequently, the heat sources here are mainly due to thermoelastic coupling. This is corroborated by the fact that no significant mechanical hysteresis is observed in terms of the strain-stress relationship.

In the following, these results are compared to those obtained for SBR50. Results are first discussed qualitatively. They are then analysed quantitatively in order to evaluate accurately the level of mechanical dissipation depending on the maximum stretch ratios applied. Figure 5 presents the mechanical response of SBR50. Each mechanical cycle exhibits a hysteresis loop, and stress softening is observed for each series. This stress softening phenomenon is well known in filled rubbers. It is referred to as "the Mullins effect" in the literature. In the present study, the Mullins effect is not investigated. Only the third cycle of each series is considered for our analysis. These cycles are considered as mechanically stabilized in terms of both stress softening and residual strain. It should be noted that no significant increase in residual strain is observed between the second and third cycles, meaning that this residual strain can be seen as a type of damage associated with stress softening. It should be noted also that the residual strain reaches 30% for the maximum stretch ratio applied.

Figure 6 gives the heat source *versus* the stretch ratio for each third cycle for SBR50. Figure 6(a), (b), (c) and (d) present the results for $\lambda_1 = 2$, $\lambda_2 = 3$, $\lambda_3 = 4$ and $\lambda_4 = 4.5$, respectively. These figures show that the heat sources exhibit a load-unload dissymmetry. This is clearly shown by the comparison between the heat sources produced on loading and the absolute value of the heat source absorbed on unloading. This reveals that mechanical dissipation is produced. Here, the mechanical dissipation is only due to viscosity and not to any damage. This viscosity is mainly due to the high proportion of filler (50 phr, compared with 5 phr for SBR5).

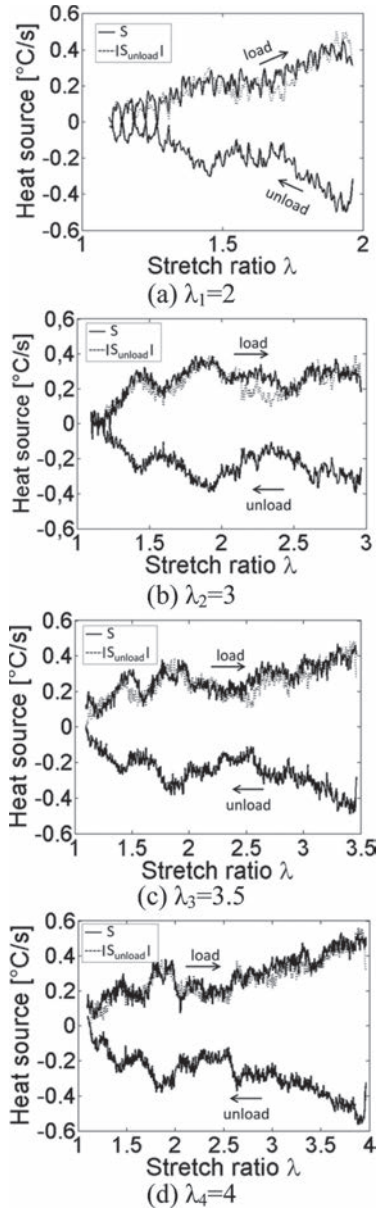

Figure 4. Heat source *versus* stretch ratio for the third cycle of each of the four series for SBR5. The dotted line corresponds to the absolute value of the heat source during unloading.

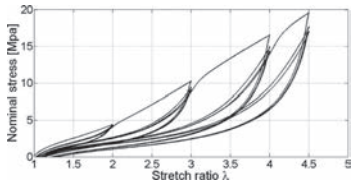

Figure 5. Mechanical response for SBR50.

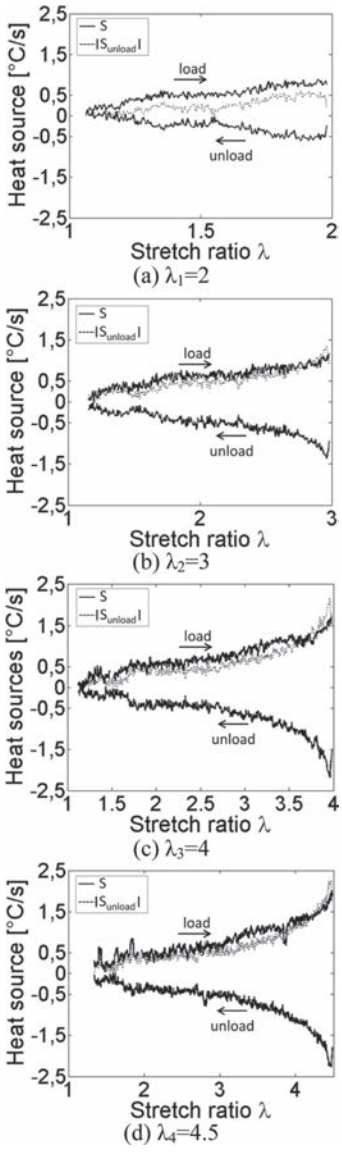

Figure 6. Heat source *versus* stretch ratio for the third cycle of each of the four series for SBR50. The dotted line corresponds to the absolute value of the heat source during unloading.

At this stage of the present study, several remarks can be formulated to analyse the results quantitatively. These remarks concern the mechanical dissipation deduced from the calorimetric response of the material. To this purpose, Figure 7 gives four different types of diagram that

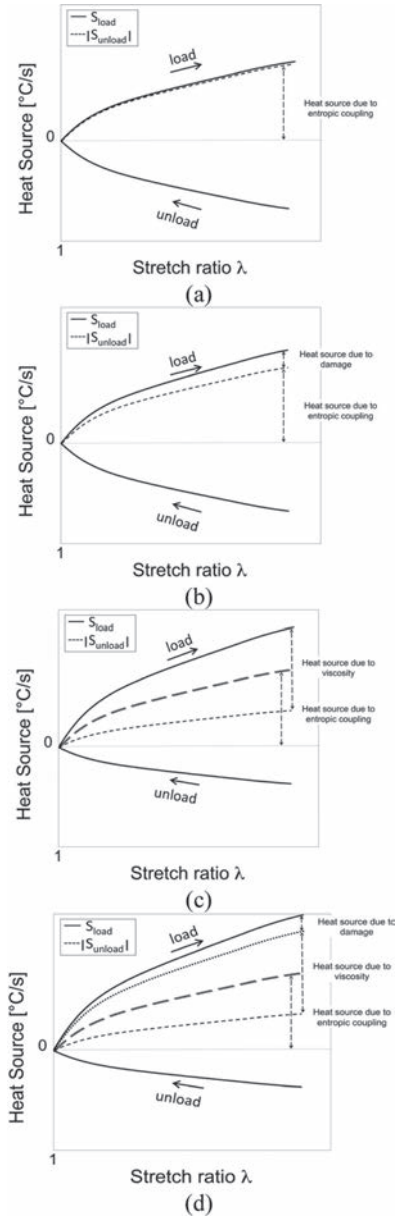

Figure 7. Schematic evolution: heat source *versus* stretch ratio for entropic behaviour (a), with damage occurring upon loading (b), with viscosity (c), with damage and viscosity (d).

can be obtained according to the nature of the rubber behaviour considered.

The contribution of the physical mechanisms involved in the deformation of rubber to the heat produced at each mechanical cycle leads us to consider various elementary calorimetric behaviours. These calorimetric behaviours are illustrated in Figure 7. Figure 7(a), (b), (c) and (d) give the calorimetric responses of purely entropic behaviour without mechanical dissipation, with damage occurring on loading, with viscosity, and with viscosity and damage, respectively.

For purely entropic behaviour (Fig. 7(a)), no dissipation occurs during the mechanical cycle. The heat source corresponds to the thermoelastic coupling term only. The variations in the heat source during loading (s_{load}) and unloading (s_{unload}) in absolute value are superimposed. Consequently, the heat produced on loading is equal to that absorbed during unloading at each stretch ratio considered. This calorimetric response is observed for SBR5, i.e. for weakly filled SBR (see Fig. 4). Figure 7(b) gives the response for entropic material with damage occurring during loading. This is not the case of Mullins softened SBR50. Obviously, this is more debatable for the first cycle of each series, even if the Mullins effect is mainly observed in filled, and therefore viscous, rubbers. Figure 7(c) gives the response for entropic and viscous material. This calorimetric response corresponds to that of Mullins softened SBR50 and provides the modelling of the results shown in Figure 6. Figure 7(d) gives the response for entropic and viscous material that is damaged during loading. It should be noted that this analysis applies only for the first cycle in filled rubber. The consequences of the Mullins effect on the calorimetric response are studied in a future paper under review for publication.

This interpretation framework, especially Figure 7(c), leads to a quantitative analysis of the calorimetric response of SBR50 by calculating the difference between the heat produced on loading and that absorbed during unloading. This leads us to calculate first $A_n = \int s_{load}\, dt$, then $B_n = \int s_{unload}\, dt$ and finally $C_n = \int s_{load}\, dt + \int s_{unload}\, dt$. All of these quantities are expressed in °C. The heat corresponding to the mechanical dissipation over one mechanical cycle H_{d1} (in J/m^3) is calculated by multiplying C_n by the product $\rho C_{E,Vk}$. Table 2 gives the results obtained; they are summarized in the diagram in Figure 8. As shown in this figure, heat sources absorbed and produced increase quasi-linearly with the maximum stretch ratio during stabilized cycles. It should be noted that it is not the case for materials whose microstructure significantly evolves during the mechanical cycle, typically crystallisable rubbers (Samaca Martinez et al., 2013a,b). Moreover, the higher the stretch ratio, the higher the heat sources produced due to mechanical dissipation. These results constitute an interesting way to validate or enhance constitutive equations.

Table 2. Heat calculated for SBR50.

	Cycle 3 $\lambda = 2$	Cycle 3 $\lambda = 3$	Cycle 3 $\lambda = 4$	Cycle 3 $\lambda = 4.5$
$A_n = \int S_{load}\, dt$ (°C)	0.828	2.360	4.300	5.080
$B_n = \int S_{unload}\, dt$ (°C)	–0.628	–1.868	–3.280	–4.140
$C_n = A_n + B_n$ (°C)	0.200	0.492	1.020	0.94
H_{d1} (J/m^3)	0.328	0.814	1.710	1.560

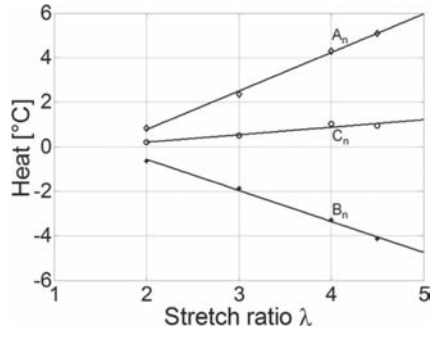

Figure 8. Heat *versus* the maximum stretch ratio reached for the third cycle of each of the four series for SBR50.

4 CONCLUSION

Calorimetric effects during SBR deformation processes were investigated using IR thermography measurements, the framework of the thermodynamics of irreversible processes and the heat diffusion equation. More particularly, the effects of the addition of carbon black fillers on the calorimetric response were studied. SBR was tested under cyclic tensile loading conditions. In the present work, only the stabilized response is analysed, i.e. the calorimetric signature of the Mullins effect is not studied here. Results show that the less-filled SBR exhibits purely entropic behaviour, meaning that no mechanical dissipation is detected. The heat produced and absorbed is the same on loading and unloading at any stretch ratio. The SBR filled with 50 phr of carbon black behaves as an entropic and viscous material. The mechanical dissipation was calculated. It increases quasi-linearly with the stretch ratio. A simplified framework is proposed to discuss the nature and the identification of the

mechanical dissipation. This experimental result is promising for the validation or enhancement of constitutive equations.

ACKNOWLEDGEMENTS

The authors would like to acknowledge the "Manufacture Française des Pneumatiques Michelin" for supporting this study. The authors also thank D. Berghezan, F. Vion-Loisel and E. Munch for their fructuous discussions.

REFERENCES

Boccara, N. 1968. Les principes de la thermodynamique classique. *Presses Universitaires de France.*

Chrysochoos, A. 1995. Analyse du comportement des matériaux par thermographie Infra Rouge. *Colloque Photomécanique.*

Chrysochoos, A. & Louche, H. 2000. An infrared image processing to analyse the calorific effects accompanying strain localisation. *Int J Eng Sci*, 38: 1759–1788

Chrysochoos, A., Huon, V., Jourdan, J., Muracciole, J.-M., Peyroux, R. & Wattrisse, B. 2010. Use of full-Field digital image correlation and infrared thermography measurements for the thermomechanical analysis of material behaviour. *Strain*, 46: 117–130.

Diani, J., Fayolle, B. & Gilormini, P. 2009. A review on the Mullins effect. *European Polymer Journal*, 45: 601–612.

Favier, D., Orgéas, L., Vacher P., Meunier, L. & Chagnon, G. 2008. Mechanical experimental characterization and numerical modelling of an unfilled silicone rubber. *Polymer Testing*, 27: 765–777.

Mullins, L. 1948. Effect of stretching on the properties of rubber. *Rubber Chemistry and Technology,* 21: 281–300.

Germain, P., Nguyen, Q.S. & Suquet, P. 1983. Continuum thermodynamics. *J. Appl. Mech.,* 50: 1010–1020.

Samaca Martinez, J.R., Le Cam, J.-B., Balandraud, X., Toussaint, E. & Caillard, J. 2013a. Thermal and calorimetric effects accompanying the deformation of natural rubber. Part 1: thermal characterization. *Doi: 10.1016/j.polymer.2013.03.011.*

Samaca Martinez, J.R., Le Cam, J.-B., Balandraud, X., Toussaint, E. & Caillard, J. 2013b. Thermal and calorimetric effects accompanying the deformation of natural rubber. Part 2: quantitative calorimetric analysis. *Doi: 10.1016/j.polymer.2013.03.012.*